Synchronization of main Global Electric Circuit generators from ground-level electric field Ez at three distant locations on the globe at middle and high latitudes

M. Kubicki[1]*A. Odzimek[1] , N.G. Kleimenova[2] , O.V. Kozyreva[2], M. Neska[1]

[1]Institute of Geophysics, Polish Academy of Sciences (IGF PAS), Warsaw, 01-452 Poland
[2]Schmidt Institute of Physics of the Earth, Russian Academy of Sciences, B. Gruzinskaya 10, Moscow 123995, Russia

ABSTRACT: The ground-level vertical atmospheric electric field E_z is affected by processes taking place in the Earth's atmosphere, ionosphere and magnetosphere. In this work we present our further attempt to check the synchronization of the signals in E_z due to main generators operating in the Global Electric Circuit (GEC) which create this electric field, from simultaneous measurements at three distant locations: Hornsund in the Arctic, Spitsbergen (77°00 ′N, 15°32′E) - HRN, Arctowski station in the South Shetland Islands (62°09′S, 58°25′W) - ARC, and mid-latitude Swider (near Warsaw) station, Poland (52°07′N, 21°14′E) - SWI. We consider that apart from the cloud generator, which is assumed to be responsible for maintaining the field globally, magnetospheric effects in E_z are present at Hornsund. At Swider, as a mid-latitude land station, the E_z is also affected by local thermal convection generator. We studied the diurnal variation of E_z for selected days of fair-weather conditions and low aerosol concentration simultaneously at these two or three sites.

INTRODUCTION

In the GEC, the main operating generators are: the cloud generator (thunderstorm and shower cloud), the magnetospheric generator associated with magnetospheric-ionospheric (M-I) plasma convection processes and Birkeland currents (FACs). These generators can changed its parameters, i.e. the amplitude of the diurnal variation depending on geographic location and time. The magnetospheric generator dominates in polar regions [*Tzur and Roble*, 1986], and the cloud generator in the low latitude region. These generators are manifested in the near-surface electric field E_z, with different weights depending on the measurement localization [e.g., *Michnowski*, 1998; *Tinsley and Heelis*, 1993]. Statistic analysis of the electric current and field in the magnetosphere, ionosphere and atmosphere confirm the existence of M-I coupling, especially during periods of high geomagnetic activity. However, for individual cases the electric coupling can be very complicated. Thus it is necessary to take into account the position of the measuring point with respect to the generators and determine the course of daily global thunderstorm activity which can even differ significantly from the Carnegie curve. The horizontal electric field maps from the magnetosphere to ionosphere downward, and affects total overhead ionospheric potential and then the ground-level electric field E_z [e.g., *Tinsley and Heelis*, 1993; *Odzimek et al.*, 2011]. One can assume that on the basis of measurements at several locations the daily variation of the main generators on the globe can be identified. In this analysis one should take into account the impact of local effects, convection and atmospheric turbulence especially at land stations and surface aerosol concentrations in polar and mid-latitudes region. The present paper discusses methods of determination of the daily variability of main GEC generators and verification of obtained results.

*Corresponding author, swider@igf.edu.pl, Postal address: Ksiecia Janusza 64.,Warsaw, 01-452 Poland

Figure 1: Left: The atmospheric electricity station. Equipment for measuring, recording and transmission of the vertical component of electric field E_z. Right: Rotating-dipole sensor for E_z measurements.

INSTRUMENTATIONS AND DATA

We analyzed variations of the vertical component of the electric field E_z measured by a rotating dipole field-mill for the interval of two years, 2012-2013. The system for measurements of the electric field strength near ground level is a rotating-dipole type sensor of frequency bandwidth from 0 to 10 Hz, sensitivity of 2 V/m, amplitude range of ± 750 V/m, and output voltage ± 3.5V. The system requires 12 V buffer power supply [*Berlinski et al.*, 2007]. In addition, near-ground aerosol concentration was measured, in the size range from 3 nm to 3 μm. This measurement is performed using an automatic ultrafine aerosol counter CPC 3025. Meteorological observations (temperature, pressure, humidity, cloudiness, cloud type, wind speed and direction, insolation, etc.) were also performed automatically or traditionally. All instruments have been installed away from local anthropogenic sources. Data were recorded synchronously from the three observation sites: ARC, HRN and SWI. The sampling frequency was one second. The data logger was a unique internet address (IP), allowing communication and control via internet and data download as well as data visualisation, and together with the buffer power supply was installed in a portable container (0.5m x 1m x 0.6 m dimensions) enabling easier installation and field measurements (Figure 1). The electric field mill was mounted 2.5 m about the ground surface in SWI and HRN, and 1.5 m in ARC. The three stations: ARC, HRN, SWI now create the Polish atmospheric electricity observation network. We have selected 20 fair-weather and low aerosol concentration days from the period 2012-2013 for stations ARC, HRN, SWI. Only 8 cases the fair weather was simultaneously at HRN and SWI, for 4 cases at ARC, HRN, SWI. We analyse in this paper only 3 individual cases. The overhead ionospheric potential due to the ionospheric convection (magnetospheric generator) V_i, is calculated from the Weimer model [*Weimer*, 1995, http://ccmc.gsfc.nasa.gov/cgi-bin], solar wind parameters and interplanetary magnetic field (IMF) data have been obtained from the NASA OMNI database (http://omniweb.gsfc.nasa.gov), auroral oval images from OVATION data (http://sd-www.jhuapl.edu), maps of the ionospheric convection from the Super Dual Auroral Radar Network (SuperDARN) (http://superdarn.jhuapl.edu), and IMAGE magnetic data (http://www.ava.fmi.fi/image).

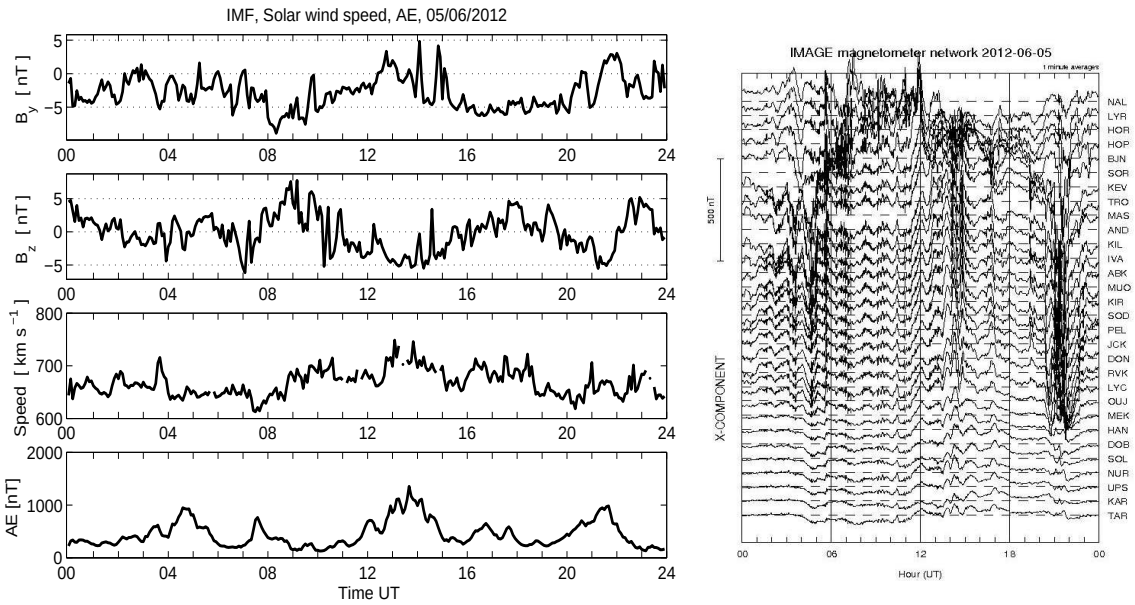

Figure 2: Left: The interplanetary magnetic field (IMF), solar wind speed and magnetic activity index associated with auroral electrojets (AE-index). Right: Magnetogram of X-component for the IMAGE Scandinavian stations on 05.06.2012.

RESULTS AND DISCUSSION

On 5 June 2012, the IMAGE Scandinavian magnetometer network recorded three substorms; it was a day of moderate geomagnetic activity $K_p = 4$, (Figure 2, right panel). The substorm at 04-06 UT is observed at polar latitudes and auroral zone and the substorm at 13-14 UT started in the auroral zone and moved to polar latitudes. The substorm at 21-22 UT started in polar region and propagated downward to middle latitudes. The solar wind parameters and interplanetary magnetic field (IMF) are presented in Figure 2, left panel. The IMF B_y component was negative most of the day. During the first substorm a small negative impulse in the IMF B_z component occurred, in the second substorm an impulse directed toward positive values. Only during the substorm on 21-22 UT the IMF B_z component changed sign from negative to positive, in this day the solar wind speed was almost constant. In Figure 3 the diurnal variations of the E_z at stations SWI (right panel) and HRN (left panel) are shown. For comparison the variations of the main generators on individual days in different locations are normalized observed surface electric field E_z according to the formula: $E_{z(zn)} = E_z/E_{z(avg)}$ where $E_{z(avg)}$ is the daily mean average. Figure 3 (right panel, center) show normalized $E_{z(zn)filter}$. The curve was created from the subtraction of smoothed (Butterworth two-order lowpass filter, cutoff time 6 h) observed E_z in SWI and local thermal convection generator, and is meant to represent approximately the diurnal global lower atmospheric cloud generator. The method assumes that the variation denoted by C (Figure 3) can be compatible with global electrified cloud activity on individual day. This was partly confirmed experimentally in the [*Nieckarz et al.*, 2009; *Golkowski et al.*, 2011]. The local thermal convection generator at SWI station ($Gen.con$) was calculated statistically on the basis of measured surface electric field E_z on days with strong thermal convection in year 2012. The observed E_z at HRN in Figure 3 (left panel, top) consists of two main components: due to the magnetospheric and cloud generator. Figure 3 (left panel, center) presents the magnetospheric generator

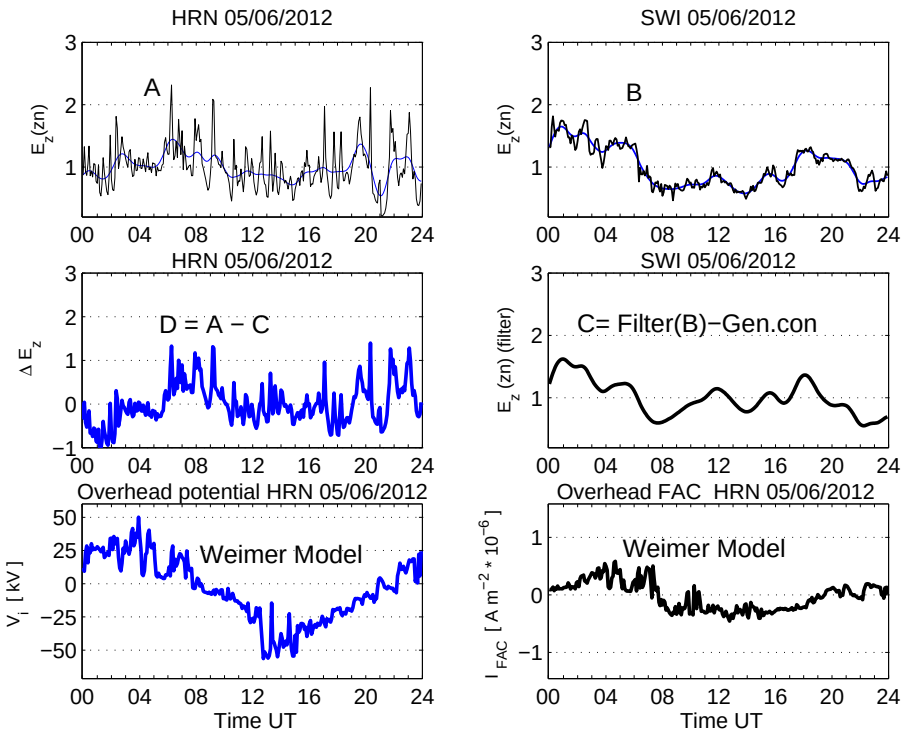

Figure 3: Normalized diurnal variation of the near-surface electric field E_z, right panel: top - observed $E_{z(zn)}$ in SWI , center - the $E_{z(zn)}$ observed in SWI, smoothed, minus the local thermal convection generator (not shown). This obtained curve should equal the low atmospheric cloud generator, bottom - overhead field aligned currents (FACs) calculated with the Weimer model, left panel: top - $E_{z(zn)}$ observed in HRN, center - diurnal variation of the magnetospheric generator ΔE_z taken as the observed electric field E_z in HRN minus the low atmospheric cloud generator from SWI, bottom - overhead ionospheric convection potential V_i calculated with Weimer model, on 05.06.2012. The letters A, B, C, D represent the individual curves.

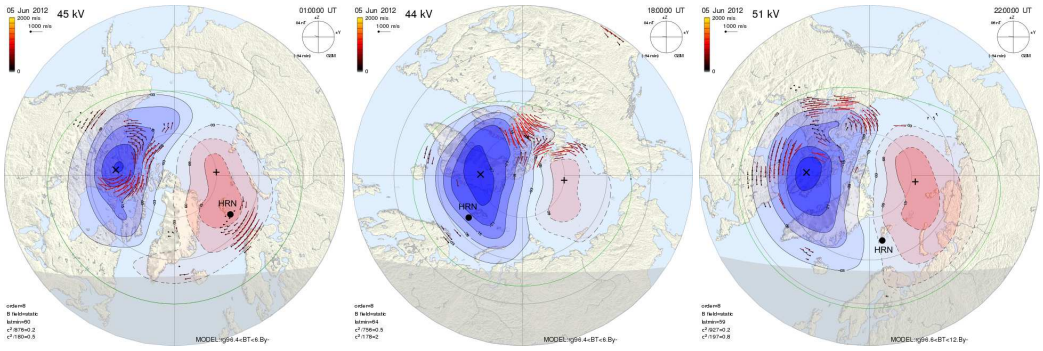

Figure 4: Convection electric potential map of ionosphere from SuperDarn on 01 UT, 18 UT, 22 UT for 05.06.2012.

ΔE_z obtained by the substraction of the cloud generator (from observations at SWI) from the observed E_z

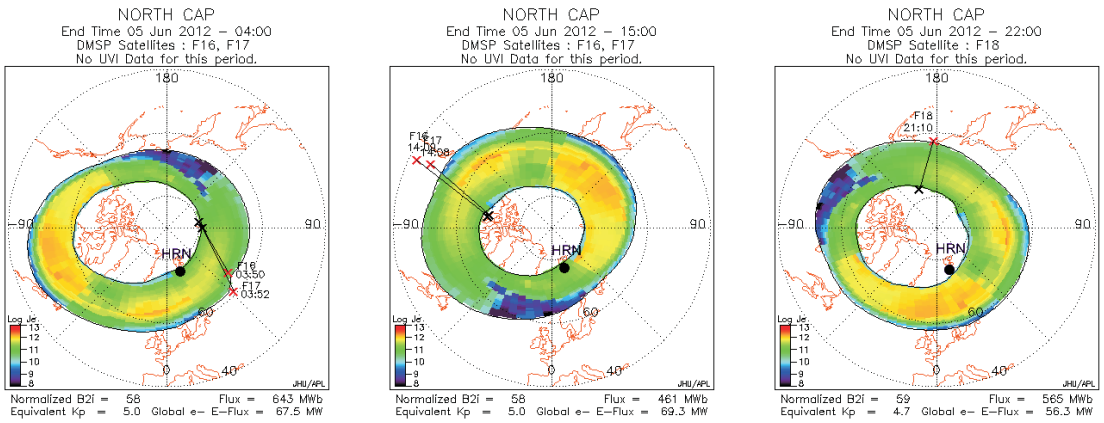

Figure 5: Localisation of the Horsund (HRN) station to the auroral oval on 04 UT, 15 UT, 22 UT on 05.06.2012.

variation at HRN. Finally, we can compare the resulting curve ΔE_z (HRN) with the overhead ionospheric potential V_i obtained from the Weimer model, as the overhead ionospheric potential represents stationary effects of the ionospheric convection, or the magnetospheric generator, in E_z. Figure 3 (right panel, bottom) shows overhead Birkeland currents (FACs) calculated from the Weimer model. The correlation of these two parameters is not significant. From 00-05 UT the variations of these parameters were opposite, from 05 to 08 UT the curves are more similar. From 09 UT the ΔE_z curve was characterized by large fluctuations around the average value of nearly zero. From this period the overhead potential V_i was negative and significantly varies (09-21 UT). The FAC current from 00 to 05 UT was positive and inflowing to the ionosphere increasing the overhead potential. The fluctuations occurring in ΔE_z and V_i may be due to an electrojet flowing over HRN.

Figure 4 shows maps of the ionospheric convection map potential [*Ruohoniemi and Baker*, 1998] based on SuperDARN radar observations on 05 June 2012. We used these maps to identify the location of the observed station HRN in relation to observed ionospheric convection patterns. At 01UT HRN was located in the positive convection cell, near to its center i.e. the maximum value of the convection electric potential, at 01 UT HRN was under negative convection cell and at 22 UT HRN was located on the boundary of the positive cell, almost between positive and negative cells. The diurnal variation the overhead ionospheric convection potential V_i obtained from Weimer model is consistent with the electric potential of the ionosphere by the SuperDARN map potential technique. Figure 5 presents the position of the Hornsund station (HRN) on the background auroral oval on 05 June 2012. During this day the HRN was located within of auroral oval or on its poleward boundary. The objective of this step is not to verify the SuperDARN map and Weimer model but verification of our method of separation of the main generators in the GEC. The lack of correlations between the V_i and ΔE_z in HRN station may be due to the fact that convection models do not take into account all ionospheric currents during disturbed magnetic days [*Frank-Kamenetsky et al.*, 2012]. In addition, the ionospheric potential map obtained by the map potential technique may not be an accurate representation of the V_i for the case of large magnetic activity [*Shepherd*, 2007]. These factors may cause difficulties in identifications of the overhead potential V_i and the magnetospheric generator ΔE_z in Hornsund.

Figure 6 shows variations of the IMF (left panel) and diurnal fluctuations of the magnetic X compo-

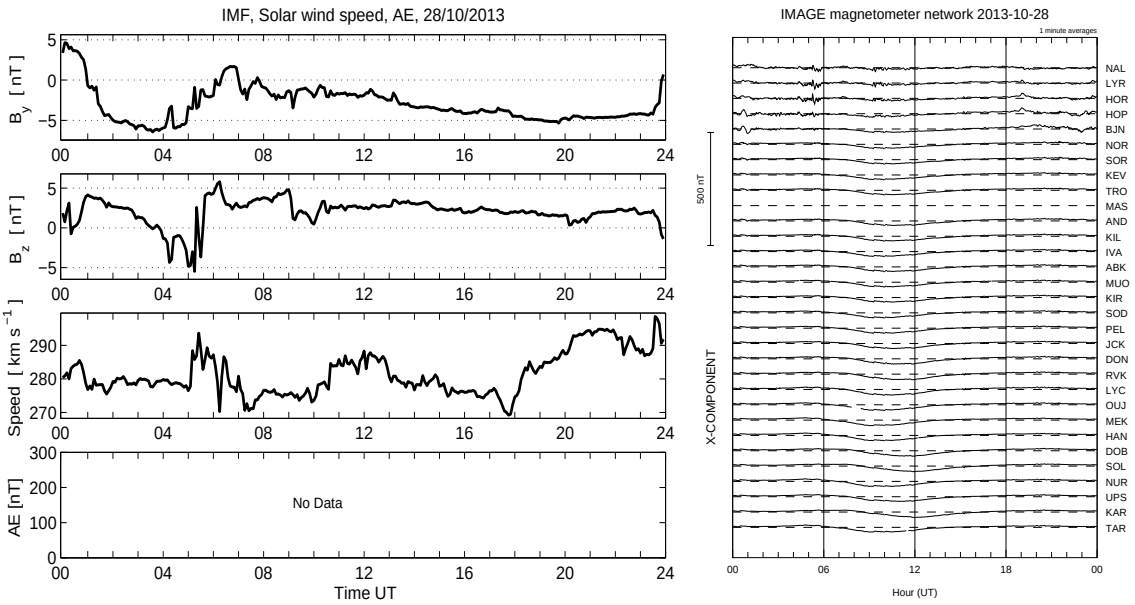

Figure 6: The interplanetary magnetic field (IMF), solar wind speed and magnetic activity index associated with auroral electrojets (AE-index); magnetogram X-component for Scandinavian stations on 28.10.2013.

nent (right panel) from the IMAGE network on 28 October 2013. On this day the magnetic activity index was $K_p = 1$. In auroral and polar cap zone there was no substorm and no intensive electrojet over HRN. The interplanetary magnetic field B_y component was negative for most of the day. The IMF $B_z > 0$ during that day, only 03-06 UT B_z component changed the sign. The solar wind speed increased suddenly about 05 UT. However, this increase was minor (about 10 km s^{-1}). On the 28 October 2013 were magnetically quiet conditions. Figure 7 summarizes the analysis of observed E_z for HRN and SWI stations and calculated ΔE_z i V_i for 28 October 2013. Description of each parameters is the same as shown in Figure 3. Curves ΔE_z (Figure 7, left panel, center) and V_i (Figure 7, left panel, bottom) are similar. On this basis, it can be assumed that the presented method can be used on this separation diurnal variations of magnetospheric and thunderstorm /cloud generators by measuring electric field in near-surface E_z in two localizations. This method is applicable on the magnetic quiet days, in the disturbed days is currently difficult to verify. If the choice for the location of measurements ensures minimisation of local effects, separation of the main generators GEC in the E_z may not be complicated [e.g *Burns et al.*, 2005].

Simultaneous E_z variations at three sites: ARC, HRN, SWI during fair weather conditions

Figure 8 shows simulations variations of the surface electric field E_z in three stations ARC, HRN, SWI in fair-weather conditions and interplanetary magnetic field IMF on 27 September 2013. During the two years of continuous measurements (2012-2013) at ARC only 4 selected days were fair-weather day also at HRN and SWI. The 27 September 2013 there was quiet magnetic activity $K_p = 0 - 1$, and the IMAGE network did not recorded strong electrojet in the ionosphere. The IMF B_z and B_y components changing slowly in the range of $\pm$ 2nT. The average speed of the solar wind was 310 km s^{-1} (Figure 8, right panel). The curve ARC contains the least fluctuation in comparison with the curves at HRN and SWI (Figure 8, left panel). This may be the result of the location of the ARC station in the area where the impact of local effects

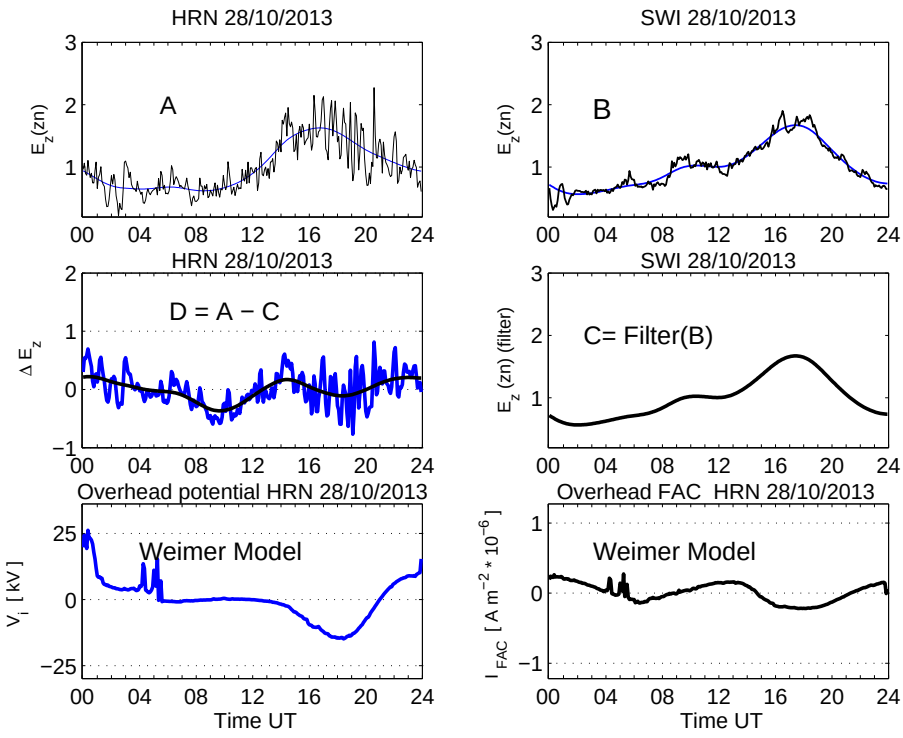

Figure 7: Normalized diurnal variation of the near-surface electric field E_z, right panel: top - observed $E_{z(zn)}$ in SWI , center - the $E_{z(zn)}$ observed in SWI, smoothed, minus the local thermal convection generator (not shown). This obtained curve should equal the low atmospheric cloud generator, bottom - overhead field aligned currents (FACs) calculated with the Weimer model, left panel: top - $E_{z(zn)}$ observed in HRN, center - diurnal variation of the magnetospheric generator ΔE_z taken as the observed electric field E_z in HRN minus the low atmospheric cloud generator from SWI, bottom - overhead ionospheric convection potential V_i calculated with Weimer model, on 28.10.2013. The letters A, B, C, D represent the individual curves.

is small. Additionally, the location of the Arctowski station is usually away from the Southern Hemisphere ionospheric convection and therefore it can be assumed that the effects of magnetospheric generators can be neglected in days with low magnetic activity. Therefore, the variation of cloud generator as obtained by the SWI station we compared with the variations of E_z at ARC. Good agreement of all curves E_z occurs at night, 00-03 UT, during 10-16 UT variations differ significantly. The HRN and SWI are characterized by large fluctuations. An extended analysis of this case will be made using SuperDARN, OVATION data base when they become available. Analysis of simultaneous variations of E_z of the two distant polar regions is Vostok (Antarctic region) station and Horsund (Arctic region) was presented in the work [*Frank-Kamenetsky et al.*, 2012].

CONCLUSIONS AND FUTURE WORK

1. The coupling between the magnetopsheric-ionospheric current system with the atmospheric one seems to be complicated in individual cases.

2. The effect of the magnetospheric generatorΔE_z as obtained from the measured electric field E_z is

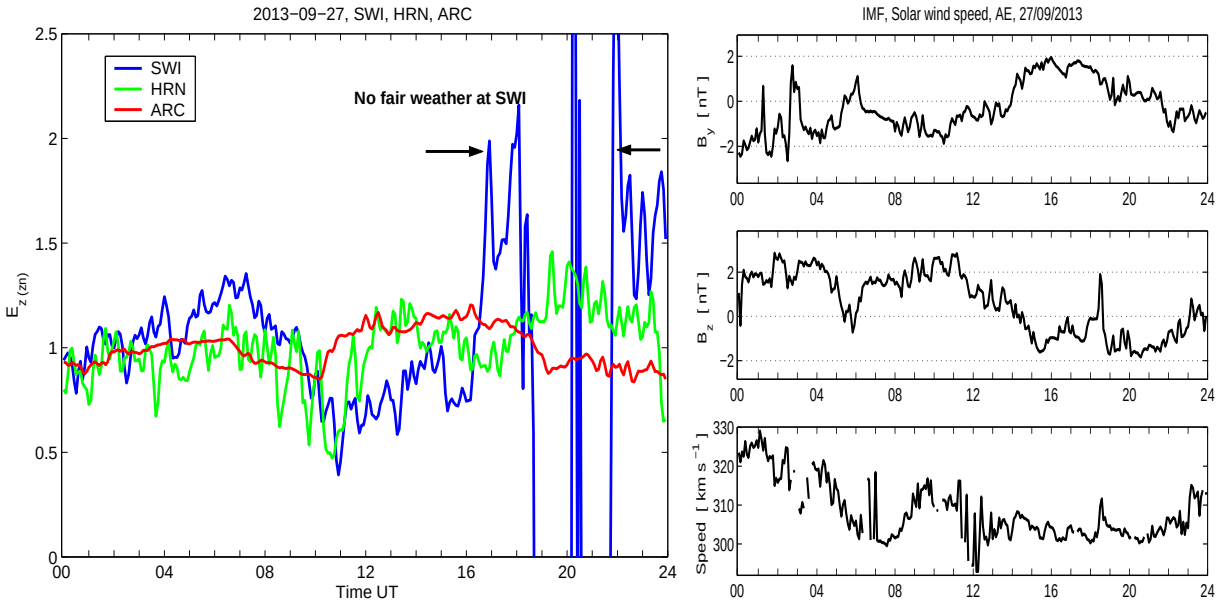

Figure 8: Left, Normalized diurnal variation of the near-surface electric field $E_{z(zn)}$ at SWI, HRN, ARC. Right, The interplanetary magnetic field (IMF), solar wind speed on 27.09.2013

highly variable in the morning and evening hours, similarly V_i, hoverer these changes are not always consistent with each other.

3. The relation between the overhead potential V_i calculated from ionospheric models (e.g. Weimer model) and the magnetospheric generator ΔE_z determined from E_z measurements depend on the IMF, plasma convection and the location of HRN in relation to polar electrojets. The relation becomes stronger for particular configurations of the magnetospheric-ionospheric current system.

In the near future in the verification of the presented method of separation of the main generators data for individual day storm activity on the Global Lightning Dataset (GLD360) [*Said et al.*, 2010] will be used. The variation of E_z at middle latitudes (SWI), high latitudes (ARC) will also be compared with the global thunderstorm activity (diurnal variation of average number of lightning strikes per hour and average current per hour) from GLD360 on individual days. Initial analysis was done by [*Golkowski et al.*, 2013]. The knowledge of individual diurnal variation of global thunderstorm activity is important because it affects the determination of the magnetospheric generator. The E_z measured at the tree sites will be used to study the penetration of electric fields from the magnetosphere to mid and low latitudes during strong magnetic storms [e.g., *Kleimenova et al.*, 2013]. The experience resulting from the measurements in three sites on the globe (Polish Atmospheric Electricity Network) indicate the need of increasing the number of measuring points as fair weather conditions rarely occurs simultaneously in all points in this global network simultaneously.

ACKNOWLEDGMENTS: This work is supported by Polish National Science Centre (NCN), grant number 2011/01/B/ST10/07118. We gratefully the SuperDARN Web for providing the ionospheric potential map, OVATION, OMNI and IMAGE Web.

References

Berlinski, J., G. Pankanin, and M. Kubicki, Large scale monitoring of troposphere electric field, in *Proceedings of the 13th International Conference on Atmospheric Electricity*, vol. 1, 2007, ICAE2007, August 13-18, Beijing.

Burns, G. B., A. V. Frank-Kamenetsky, O. A. Troshichev, E. A. Bering, and B. D. Reddell, Interannual consistency of bi-monthly differences in diurnal variations of the ground-level, vertical electric field, *J.Geophys.Res.*, *110*, 2005.

Frank-Kamenetsky, A., A. Kotikov, A. Kruglov, B. Burns, N. Kleimenova, O. Kozyreva, M. Kubitski, and A. Odzimek, Variations in the near-surface atmospheric electric field at high latitudes and ionospheric potential during geomagnetic perturbations, *Geomagnetism and Aeronomy*, *5*, 629–638, 2012.

Golkowski, M., M. Kubicki, M. Cohen, A. Kulak, and U. Inan, Estimation of global lightning activity and observations of atmospheric electric field, *Acta Geophys. Pol.*, *59*, 183–204, 2011.

Golkowski, M., M. Kubicki, and B. Brady, Assessing fundamental drivers of the global electric circuit and the potential role of earthquakes, in *Proceedings of the American Geophysical Union Fall Meeting*, vol. NH31B-1609, 2013, AGU Fall 2013, San Francisco, USA, 9-13 December 2013.

Kleimenova, N. G., O. V. Kozyreva, S. Michnowski, and M. Kubicki, Influence of geomagnetic disturbances on atmospheric electric field Ez variations at high and middle latitudes, *J.Atmos. Sol. Terr. Phys.*, *99*, 117–122, 2013.

Michnowski, S., Solar wind influences on atmospheric electricity variables in polar regions, *J.Geophys.Res.*, *103*, 13,939–13,948, 1998.

Nieckarz, Z., A. Kulak, S. Zieba, M. Kubicki, S. Michnowski, and P. Baranski, Comparison of global storm activity rate calculated from Schumann resonance background components to electric field intensity Eoz, *Atmospheric Research*, *91*, 184–187, 2009, 13th International Conference on Atmospheric Electricity.

Odzimek, A., M. Kubicki, M. Lester, and G. A., Relation between the superdarn ionospheric potential and ground electric field at polar station hornsund., in *Proceedings of the 14th International Conference on Atmospheric Electricity*, 2011, 7-12 August 2011, Rio de Janeiro, Brazil.

Ruohoniemi, J., and K. Baker, Large-scale imaging of high-latitude convection with Super Dual Auroral Radar Networ HF observations, *J.Geophys.Res.*, *103*, 20,797–20,811, 1998.

Said, R. K., U. S. Inan, and K. L. Cumminus, Long-range lightning geolocation using a VLF radio atmospheric waveform bank, *J.Geophys.Res.*, *115*, 2010.

Shepherd, S. G., Polar cap potential saturation: Observations, theory, and modeling, *J.Atmos. Sol. Terr. Phys.*, 2007.

Tinsley, B. A., and R. A. Heelis, Correlations of atmospheric dynamics with solar activity. evidence for a connection via the solar wind, atmospheric electricity, and cloud microphysics, *J.Geophys.Res.*, 1993.

Tzur, I., and R. G. Roble, The interaction of a dipolar thunderstorm with its global electrical environment, *J. Geophys. Res.*, *90*, 5989–5999, 1986.

Weimer, P., Models of high-latitude electric potentials derived with a least error fit of spherical harmonic coefficents, *J.Geophys.Res.*, *100*, 19,595–19,607, 1995.